

RELAY-BASED VS. CONVENTIONAL WIRELESS NETWORKS: CAPACITY AND SPECTRUM EFFICIENCY

E. Weiss, S. Max, O. Klein, G. Hiertz and B. Walke
Communication Networks, Faculty 6, RWTH Aachen University
Kopernikusstr. 16, 52074 Aachen, Germany
erik.weiss@comnets.rwth-aachen.de

ABSTRACT

Conventional radio cells suffer from the disadvantageous distribution of the transmission rates. High transmission rates are only available in the close vicinity of the access point, whereas the distribution of mobile stations behaves complementary. Hence, the provided capacity of the access point is only partly used and the majority is wasted. This drawback will grow with the introduction of future transmission techniques, which increase the maximum transmission rates available at short distances. Therefore, it is unlikely that the traditional design of cellular radio systems can achieve the ambitious throughput and coverage requirements of fourth-generation (4G) radio networks. We propose to extend conventional multi-cellular systems by applying relay-enhanced topologies to each cell. To encourage this evolutionary step we present an analytical model to compute the upper bound capacity and the spectrum efficiency of wireless networks. Based on this analytical model the potential of conventional cellular systems is compared with relay-enhanced networks.

I. INTRODUCTION

The very high transmission rates foreseen for 4G systems in reasonable large areas appear to be unfeasible with conventional cellular architectures for two basic reasons. First, the envisioned spectrum for 4G systems will probably be located well above the 2GHz band used by the 3G systems. The radio propagation in these bands undergoes heavy signal attenuation. Second, the expected transmission rates for 4G systems are considerably higher than for 3G systems. However, coverage range of these transmission rates stays hardly the same as for legacy wireless technologies. It is well known that there is always a tradeoff between coverage range and transmission rate [1].

Consequently, it is unlikely that the ambitious throughput and coverage requirements for 4G systems can be achieved with the conventional design of cellular radio systems. However, relay-enhanced networks introducing multi-hop capabilities to cellular systems together with advanced transmission techniques and antenna technologies have the potential to fulfill the requirements of 4G systems [2]. In the context of this paper, each Access Point (AP) establishes a conventional wireless access network (a cell) and operates at a certain frequency band. Adding wireless Relay Stations (RSs) improves the conventional cell and forms a Relay-Enhanced Cell (REC) [2]. Only RSs are allowed to forward the data traffic. RSs within this work fully decode-and-forward (e.g. like wireless bridges or digital repeaters) the received information. In order to limit the device costs APs and RSs are equipped with one transmitter only. Thus, a REC represents a relay-enhanced network where all transmissions, i.e. between AP, RS and Mobile Stations (MSs) share the same frequency band.

The focus of this article is not the evaluation of a certain communication system respectively technology but to derive an upper bound capacity and the spectrum efficiency of different cell topologies, thus allowing a fair and system independent comparison between conventional cellular and advanced REC topologies.

The article is organized as follows. First, an overview about the state of the art is given. The next section introduces the envisaged REC topologies for a multi-cellular arrangement. The third section contains an overview of the analytical system model. Based on the system model, section four presents the upper bound capacity and the spectrum efficiency. Section five concludes our work and summarizes the results and major findings.

II. STATE OF THE ART

The idea to improve cellular systems with relays has been presented already in 1985 [3]. However, due to the envisaged challenges for 4G systems, nowadays the interest in relay-enhanced networks grows again. The authors of [2] present a detailed overview about the potential and challenges of relay based networks. Our work applies similar REC topologies and continues their work to compare the potential of RECs with conventional cellular systems.

Another growing research topic is the analytical capacity computing of wireless multi-hop networks. This research topic almost started with the seminal work from Gupta et al. [4]. They present the upper bound capacity of wireless ad-hoc networks by computing the throughput obtainable by each node. The main results show that, under optimal placement of nodes within a disc area and optimal selection of transmission power and traffic pattern, the throughput per MS scales with $1/\sqrt{n}$. Therefore, the authors concluded, that due to the vanishing throughput, efforts should be targeted to small networks.

In [5], Toumpis et al. present methods to compare the capacity of various transmission strategies. Their analytical model considers interference from concurrent transmissions, similar to the physical model described in [4]. Network States (NSs)

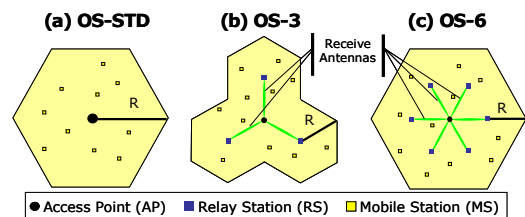


Fig. 1.: Conventional (a) and advanced REC cells

are introduced as the key element and describe successful concurrent transmissions for a wireless network at a given

time. At different times, networks may operate using different NSs. The challenge is to find an optimal schedule of all NSs that minimizes the complete transmission time and thus the resource utilization in the wireless network. The upper bound capacity is reached by exhausting the available radio resources with an optimum schedule of NSs.

This article focuses on analyzing the upper bound capacity and the spectrum efficiency of multi-cellular REC arrangements, where all transmissions in a cell share the same frequency band and apply the same transmission power.

III. SCENARIOS AND DEPLOYMENT TOPOLOGIES

The scenarios investigated within this article apply RECs in open space scenarios. The RECs consist of static RSs, allowing to apply directed receive antennas at the RSs and the AP, which amplify the signal power by an antenna gain of 11.8 dB. The REC topologies adopt two competing design goals, either maximizing the cell area or increasing the capacity and spectrum efficiency covering the same cell area.

The RECs extend conventional cell topologies, see Fig. 1. The first scenario, shown in Fig. 1(a) represents a conventional Open Space (OS-STD) scenario design consisting of one AP, only. Fig. 1(b-c) depict the REC topologies based on OS-STD with three (OS-3) and six (OS-6) additional RSs. Regarding the two design goals we distinguish between RECs extending the cell area, OS-3^A and OS-6^A and RECs focusing on capacity maximization, namely OS-3^C and OS-6^C. Table 1 lists the respective cell radii R and the covered cell areas for the different cell sizes. While Fig. 1 depicts the different cell topologies, Fig. 3 shows the applied multi-cellular arrangements of equal cell topologies. Differently colored cells indicate different frequency bands to be used within the cells.

| Scenario | Cell Area A_{Cell} | Radius R |
|-------------------|-----------------------|----------|
| OS-STD | 0.104 km ² | 200 m |
| OS-3 ^C | 0.104 km ² | 115,46 m |
| OS-6 ^C | 0.104 km ² | 100 m |
| OS-3 ^A | 0.311 km ² | 200 m |
| OS-6 ^A | 0.416 km ² | 200 m |

Table 1. Radius and resulting Cell Size

Fig. 3 (a) shows the conventional arrangement of OS-STD cells and (b, c) the multi-cellular arrangement of the RECs. The scenarios (a-c) are depicted applying three frequencies (N=3). All multi-cellular arrangements consist of one centre cell, which will be evaluated and the adjacent cells up to the first ring of co-channel cells, operating on the same frequency. The intercell-interference generated from the co-channel cells interferes the centre cell and significantly reduces the system capacity.

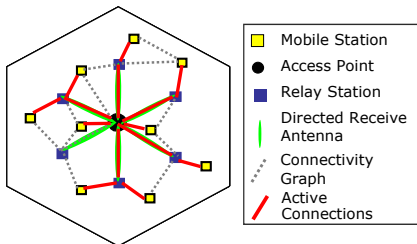


Fig. 2. Selection of Multi-hop Paths

Interference originating from co-channel cells beyond the first ring has no significant impact compared to the cells of the first ring and is neglected. The cellular arrangement of the scenarios is equal unless all cells have the same size. The only

difference is the covered cell area, see Table 1.

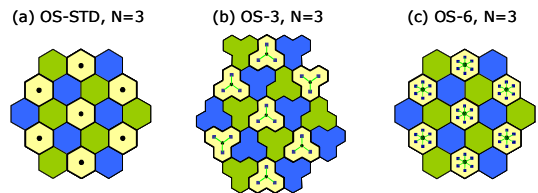


Fig. 3. Multi-cellular arrangement of conventional cells and REC Topologies, exemplified with three frequencies

The capacity of each multi-cellular arrangement is calculated by considering an increasing number of MSs. The MSs are spread randomly within the cell area. Different from the assumption in [4], we assume that each MS demands data traffic that either comes from or goes to the AP. The traffic model divides the data traffic in 10% uplink (the MS sends information to the internet via the AP) and 90% downlink traffic.

IV. SYSTEM MODEL

The system model contains the physical layer (PHY), the Medium Access Control (MAC) and the network layer. In order to acquire the capacity, the amount of resources (transmission time) consumed by transmitting a specific amount of information is determined.

The first step comprises the scenario selection, the setup of

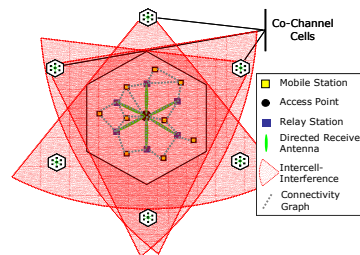


Fig. 4. Computing the Connectivity Graph under the burden of the Intercell-Interference (exemplified for three co-channel cells)

MNs and selecting the applied number of frequencies. The aim of the PHY model is to calculate the Signal to Interference plus Noise Ratio (SINR) for a set of concurrent transmissions.

The PHY model calculates the receive power considering the distance between transmitter N_i

and receiver N_j (Eqn. (1) and Table 2).

$$\frac{P_{j,Rx}}{[dBm]} = \frac{P_{i,Tx}}{[dBm]} - 20 \log_{10} \left(\frac{4\pi d_0}{\lambda} \right) - 10\gamma \log_{10} \left(\frac{d_{i,j}}{d_0} \right) \quad (1)$$

Multi-cellular mesh networks have to cope with two major interference sources. Like conventional cellular systems the co-channel cells produce intercell-interference and in addition exploiting concurrent transmissions produces intracell-interference.

In Fig. 4 a certain number of MSs are randomly distributed in the evaluated center cell. The center cell is exposed to the intercell-interference from the co-channel cells and the background noise (N). Fig. 4 depicts exemplarily the intercell-interference from the three upper co-channel cells. The experienced SINR at each receiver is calculated, as shown in Eqn. (2).

$$SINR[i, j] = \frac{P_{j,Rx}}{N + I_{Intracell}[i, j] + I_{Intercell}} \quad (2)$$

Both kinds of interference have to be considered carefully when calculating the capacity. The intracell-interference is

defined as follows. If U is a group of concurrent transmitters in a cell, the calculation of the intracell-interference experienced by the receiver N_j is calculated by summing up the received power P_{R_x} of all concurrent transmitters (3).

$$I_{\text{Intracell}}[i, j] = \sum_{k \in U, k \neq j} P_{k, R_x} \quad (3)$$

The intercell-interference originating in the first ring of co-channel cells corresponds to the sum of all concurrent transmissions in all considered co-channel cells. Let Z be the group of interfering co-channel cells and U_z denotes the group of concurrent transmissions in the co-channel cell $z \in Z$. Hence, the experienced intercell-interference can be calculated with (4):

$$I_{\text{Intercell}} = \sum_{z \in Z} \sum_{u_z \in U_z} P_{u_z, R_x} \quad (4)$$

The system model addresses the different interference sources in two steps. At first, the connectivity graph is established considering the noise and the average intercell-interference, only. The transmission conditions between all stations are evaluated and the set of potential links creates the connectivity graph.

During the second step all possible varieties of concurrent transmissions are identified, which are not exceeding the acceptable interference level at all involved receivers.

For a successful packet transmission from Node N_i to N_j , a set of four conditions has to be fulfilled. Two of them hold for any configuration of the PHY:

1. N_i must transmit only to node N_j , i.e. it cannot transmit to another node or receive at the same time.
2. N_j must receive only from node N_i , i.e. it cannot receive from another node or transmit at the same time.

The power and the SINR condition depend on thresholds specific for each MCS:

3. The received signal power P_{i, R_x} must exceed a threshold $Thres_P$ (MCS).
4. The $SINR_{i, j}$ during the transmission must be above a threshold $Thres_{SINR}$ (MCS).

| | |
|-----------------------------|---------|
| Frequency (f) | 5.5 GHz |
| Transmit Power (P_{Tx}) | 30 dBm |
| Background Noise (N) | -95 dBm |
| Antenna Gain (g_R) | 11.8 dB |
| Attenuation factor γ | 2,4 |

Table 2: Physical Parameters of the PHY

The model applies the Modulation- and Coding Schemes (MCS) known from the air interfaces of HiperLAN/2 and IEEE 802.11a [8]. Both the SINR and the power threshold depend on the MCS selected by the transmitter. We assume

the transmitter is able to determine the MCS with the highest transmission rate out of the possible schemes aiming at a packet error rate (PER) below 10%. In case connections suffer from high interference resulting in the lowest transmission rate and a PER above 10%, the considered transmission rate is reduced by the erroneous transmissions.

Applying the conditions discussed above allows for establishing the connectivity graph, see Fig. 2. The connectivity graph is the basis for the multi-hop paths and the corresponding SINR values are used to preselect a MCS for each connection. The cost of each path is measured in total transmission time. Based on the Floyd-Warshall-Algorithm the cheapest paths are calculated utilizing the inverse transmission rate of a link as respective transmission cost. The established paths form a tree structure selecting the active connections, see Fig. 2.

To calculate the maximum achievable throughput of the wireless network, an idealized MAC without any protocol overhead is assumed: Each node is omniscient and able to schedule its transmission time instantly such that no collision occurs. The idealized MAC is able to make use of spatial reuse

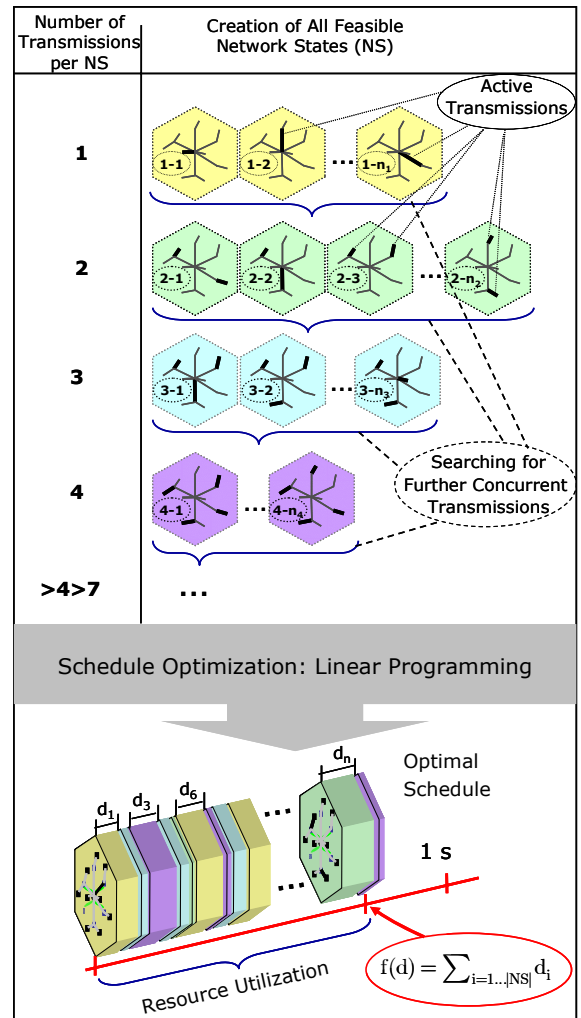


Fig. 5. Computing all feasible Network States and creating an Optimal Schedule

in the REC in a way that concurrent transmissions are possible if the PHY conditions are met. The goal of the idealized MAC is to find the optimal schedule among all possible se-

quences of (concurrent) transmissions that minimizes the occupied resources, i.e. the time needed to fulfill all transmission requests. The schedule defines who transmits (concurrently) and how long. Hence, the scheduler needs to know which transmissions can be scheduled concurrently, and what is the impact of the intracell-interference. This leads to the resulting transmission rates of each connection. This knowledge is gained by establishing a set **NS**, which contains all feasible combination of concurrent transmissions ns_i , called network state (NS) [7]. Fig. 5, exemplifies the approach. All active connections are checked, whether they can operate concurrently. The upper half of Fig. 5 shows few examples of NSs, showing all connections, but highlighting the concurrent connections.

The exhaustive generation of all feasible NSs, starts with the formulation of all NSs consisting of one transmission only. In the next step, the already existing NSs are examined whether a further concurrent transmission can be added. In this case, a new NS is created and inserted into **NS**. This step is repeated until no new NS can be generated with a concurrent transmission. The set **NS** is completed. Since the number of feasible NSs rises exponentially with the number of nodes [6], we apply the heuristics introduced in [7] to restrict the number of NSs without lowering the solution quality.

The scheduler divides the time into periodic schedule intervals of 1s length in which the same schedule applies. A schedule is defined as a list $([NS_1, d_1], [NS_2, d_2], \dots, [NS_S, d_S])$ of network states and respective application durations d_i . The second challenge is to find the optimum combination and application duration of NSs, creating an optimal schedule. A schedule is optimal if no other shorter schedule exists that fulfills all traffic requirements, as defined in matrix **T**. This optimization task is performed solving the Linear Programming (LP) instance (5) realized with the help of a commercially available optimization toolbox [9].

$$\begin{aligned}
 &\text{minimize} && f(d) = \sum_{i=1 \dots |\mathbf{NS}|} d_i \\
 &\text{under the condition} && \sum_{i=1 \dots |\mathbf{NS}|} d_i \cdot ns_i \geq \mathbf{T} \\
 &\text{and} && 0 \leq d_i \leq 1 \quad i = 1 \dots |\mathbf{NS}|
 \end{aligned} \tag{5}$$

The resulting vector $d=(d_1, \dots, d_S)$ assigns the exactly needed durations to all NSs and determines the duration of the optimal schedule.

V. ANALYTICAL RESULTS

The previous section explained the investigated scenarios and their multi-cellular arrangement. This section presents first the upper bound capacity of all scenarios and frequencies. As discussed earlier, either the cell area is kept equal or the cell area is enlarged. Besides the already mentioned three frequencies shown in Fig. 3, we also present results for larger cell arrangements with seven and twelve frequencies ($N=7, N=12$). More cells operating on different frequencies increase the distance between co-channel cells and thus, decrease the influence of the intercell-interference.

The upper bound capacity describes the maximum user data that can be transported on average, with a given number of MSs in the scenario, normalized to the maximum transmission rate [13].

The duration of an optimal schedule for a trial and a certain traffic pattern **T**, defines the normalized upper bound capacity (CAP) at 100% resource utilization. Following a Monte-Carlo approach, the positions of the MSs are varied and the upper bound capacity for each trial is calculated separately until the normalized upper bound capacity and spectrum efficiency for each topology are statistically firm.

Fig. 6 shows three sub-graphs, each represents a different number of frequencies. The left sub-graph, presents the capacity with three, the mid graph with seven and the right graph with twelve frequencies. As it can be seen, the exploitable capacity of an AP, for OS-3^A and OS-3^C is similar. The topologies with smaller cells achieve a higher capacity. With three frequencies the differences between the design goals ‘larger cells’ and ‘higher capacity’ is small but with increasing number of frequencies the differences grow.

At first the similar capacity results seems to be surprisingly, but one has to take into account that smaller cells profit from shorter connection distances but at the same time suffer from closer co-channel cells. Whereas, larger cells profit from the enlarged distance to the co-channel cell but at the same time the connection distances increases as well. If the number of frequencies grows the benefits of shorter connections become more significant as the distance to the co-channel cells. Therefore, the capacity gain of OS-6^C compared to OS-6^A with twelve frequencies is almost 3%.

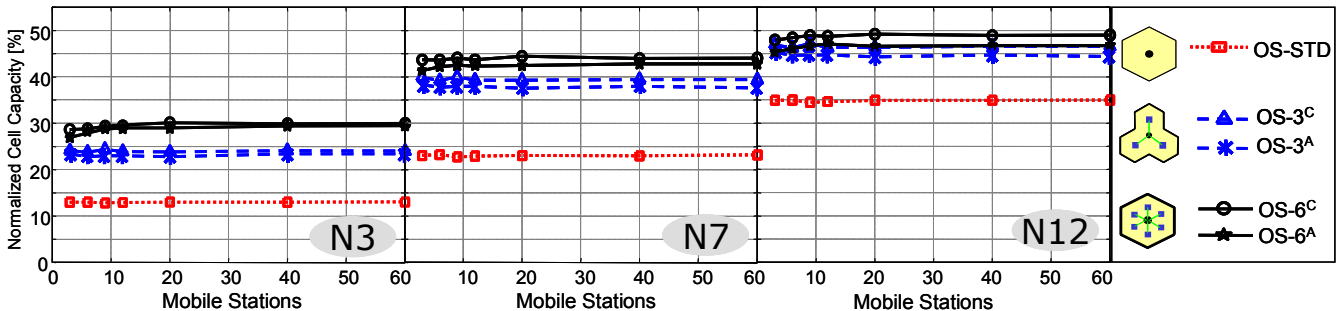


Fig. 6. Upper Bound Capacity of the cellular-based OS arrangement

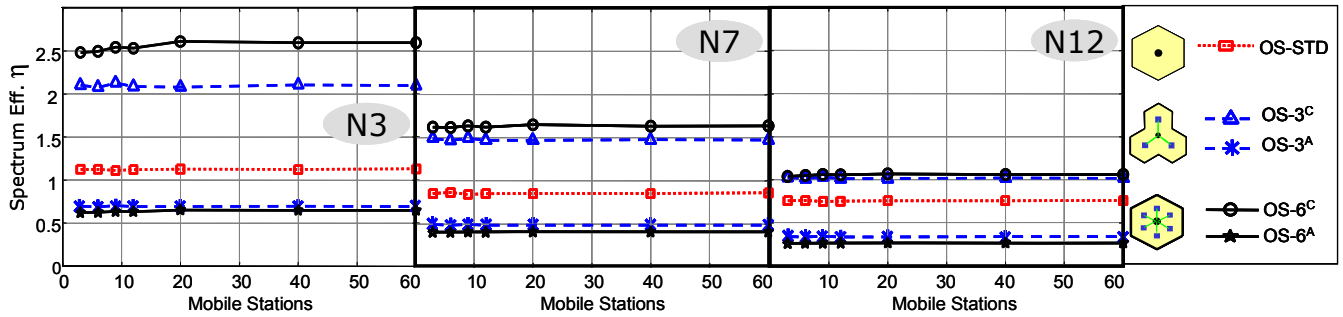


Fig. 7. Maximum Spectrum Efficiency of cellular-based OS arrangements

The conventional cell arrangement OS-STD reaches a capacity of 13% with three, 23% with seven, and 35% with twelve frequencies. The REC topologies OS-3 and OS-6 show always a higher capacity. The capacity gain with RECs is between 10-20% and is almost independent from the amount of MSs per cell.

All topologies suffer from strong intercell-interference, but REC topologies are less vulnerable. This results in a higher exploitable capacity. Consequently, REC topologies, utilizing advanced antenna techniques and concurrent transmissions, improve the system capacity, which is a mandatory precondition for 4G systems.

The spectrum efficiency η measures the amount of user data traffic that can be transmitted over a given spectrum within a certain cell area, see (6).

$$\eta = \frac{CAP}{N \cdot B_f \cdot A_{Cell}} \left[\frac{Mb/s}{MHz \cdot km^2} \right] \quad (6)$$

With $B_f = 20$ MHz bandwidth per frequency, N the number of frequencies, and A_{Cell} represents the cell area. Fig. 7 presents the system capacity with respect to the needed bandwidth and the covered cell area. This measure shows clearly the benefits of different REC topologies. The highest spectrum efficiency can be observed for OS-6^C and OS-3^C applying three frequencies. The spectrum efficiency of OS-6^C with three frequencies is lower with three frequencies, the spectrum efficiency is higher, since the system wide allocated bandwidth is smaller. Investing more frequencies increase the capacity but the gain is not commensurate with the increased spectrum.

REC topologies focusing on larger cell areas show lower spectrum efficiency than the conventional deployment. This was expected, since spreading the capacity over a larger cell area means less capacity per square meter. However, extending the cell area with RS is a reasonable approach to cover large areas with a low number of customers, e.g. at the system rollout.

VI. CONCLUSION

Nowadays, a shift away from the conventional cellular-based deployment concept is observed: In relay-enhanced networks, dedicated relay stations introduce a new dimension of flexi-

bility, which increases the system performance towards the demands of fourth-generation mobile broadband users. The expected transmission rates of fourth-generation communication systems are considerably higher than for third-generation systems. Therefore, it is unlikely that the traditional design of cellular radio systems can achieve the ambitious throughput and coverage requirements for fourth-generation systems. We propose to extend conventional multi-cellular systems by applying multi-hop topologies to each cell.

An analytical system model allowing the evaluation of the upper bound capacity and the spectrum efficiency of wireless networks has been developed and is applied to compare RECs with conventional cellular systems.

The presented results show significant capacity gains and increases in spectrum efficiency achievable with the deployment of multi-cellular REC topologies. Thus, REC topologies offer an attractive solution to accomplish the requirements of the fourth-generation mobile broadband communication systems.

REFERENCES

- [1] W. Mohr, R. Lüder, K.-H. Möhrmann, "Data Rate Estimates, Range Calculations and Spectrum Demand for New Elements of Systems Beyond IMT-2000," *Proc. 5th Int'l. Symp. Wireless Pers. Multimedia Commun.*, Honolulu, HI, Oct. 2002.
- [2] R. Pabst et al., "Relay-based deployment concepts for wireless and mobile broadband radio", *Communications Magazine*, IEEE, vol. 42, no. 9, pp. 80-89, September 2004
- [3] B. Walke, R. Briechle, "A Local Cellular Radio Network for Digital Voice and Data Transmission at 60GHz", *In Cellular and Mobile Comms. International*, p.p. 215-225, London, 1985
- [4] P. Gupta and P.R. Kumar. "The capacity of wireless networks". *IEEE Transactions on Information Theory*, IT-46(2):388-404, March 2000.
- [5] S. Toumpis and A.J. Goldsmith, "Capacity regions for wireless ad hoc networks," *IEEE Transactions on Wireless Communications*, vol. 2, no. 4, pp. 736-748, July 2003
- [6] E. Arikani "Some complexity results about packet radio transmission," *IEEE Transactions on Information Theory*, vol. 46, no 4, pp. 681-685, July 1984.
- [7] S. Max, E. Weiss, "Calculation methods for capacity estimation of wireless networks in realistic environments", *Tech. Rep., Chair of Communication Networks*, Faculty 6, RWTH Aachen University (July 2006). URL <http://www.comnets.rwth-aachen.de>
- [8] IEEE, "IEEE Wireless LAN Edition - A compilation based on IEEE Std. 802.11 1999(R2003) and its amendments", *IEEE, New York, Standard IEEE 802.11*, Nov. 2003.
- [9] <http://www.mathworks.com>